

# Surface Plasmon Resonance biosensors and Stimulated Emission Microscopy

Case studies about the interaction of  
the electromagnetic field and matter



Ádám Fekete

*Theses of the Ph.D. dissertation*

Supervisor:

Prof. Árpád Csurgay

PÁZMÁNY PÉTER CATHOLIC UNIVERSITY  
FACULTY OF INFORMATION TECHNOLOGY AND BIONICS  
MULTIDISCIPLINARY DOCTORAL SCHOOL OF SCIENCES AND TECHNOLOGY

Budapest, 2015

# 1 Introduction

The recent improvement in measurement techniques and the development of nanotechnology created new methods, new devices and new experiments, that provide us with a deeper understanding of our environment and the underlying processes. For the most part in these processes the interaction of the electromagnetic field and matter plays the most significant role. In order to study this interaction, due to the reduced dimensions and accurate measuring we have to apply quantum-classical methods.

In the past decade The Surface Plasmon Resonance (SPR) based biosensors have been widely used as label-free optical detectors. These instruments due to their high sensitivity are capable of detecting small molecules without marking them with large fluorescent molecules. -. Although the main operational principle of SPR biosensor is based on the classical electromagnetic field theory, in order to determine the parameters of matter we have to apply quantum mechanical models.

The Stimulated Emission Microscopy (SEM) specially developed for the label-free detection of molecules – is capable of imaging by using two laser pulses with different wavelengths. In the theoretical models of the microscope the electromagnetic field can be considered as classical, however the interaction itself can be accurately described by quantum mechanical principles.

While my new scientific results are interlinked, they can be grouped into three different chapters:

1. Surface plasmon resonance biosensors,
2. Stimulated emission microscopy,
3. Three dimensional representation of complex wave functions.

## 1.1 Surface plasmon resonance biosensors

High sensitivity of sensors based on SPR principles make it possible to detect the presence of even a few molecules [6, 7]. This feature makes them a very important, widely used biosensor. The sensitivity of the sensor is based on the narrow resonance in the frequency domain which is the reason why

it is so important to determine the characteristics of the sensor and its optimal parameters [8, 9]. As already mentioned further advantage of the SPR biosensors is that it can be used without fluorescent markers.

The biosensors are highly molecule-specific therefore they require a specific reset of the sensor parameters for the detection of each molecule. In the case of the Kretschmann type SPR biosensor we have to consider the reflective index of the prism, the wavelength of excitation and the thickness and the material of the metal layer. The optimal operation range is different for each biosensor that makes it costly and difficult to determine these parameters experimentally.

## 1.2 Stimulated emission microscopy

We usually use confocal microscopes or their developed versions for the observation of biological processes. In most cases we have to bind fluorescent markers to the molecule that we want to observe – giving us an indirect picture about the presence of the molecule of interest. The effect of the fluorescent molecule on the observed one can only be estimated in most of the cases because there can be an order of magnitude difference in the size of these two types of molecules.

The SEM microscope can be a solution to the above mentioned problems. It is a new label-free method with which one can observe molecules directly – without fluorescent markers. This is the reason why we have to be familiar with the quantitative characteristics of these microscopes [10, 11]. We are interested in a phenomenon where the dynamics of vibrational processes – the probability of the transitions of vibrational states – could be more dominant than the occupation probability of the stationary states. Furthermore because of the mode-locked pico- and femto-second laser excitation, the pulse in the frequency domain is broadened so we have to take more possible transitions into account at modeling.

### 1.3 Three dimensional representation of complex wave functions

Due to advancements in computer science it is possible to perform larger, more complex *ab initio* simulations, and the efficient representation simulation results have gained far more importance. [12, 13]. The interpretation of quantitative results is usually easier in three dimensions. Stereoscopic displays are widely used nowadays offering a new opportunity to represent the reality as precisely as possible. Because of the large amount of data it became important to have a tool in our hand that helps us represent the information accurately. It became a large problem that there is no representational method that could use the advantages of the stereoscopic displays.

Quantum chemical programs are usually using molecular isosurfaces ( the surface of a certain expectation value of finding probability). Although the representation of these isosurfaces are visually attractive, we get no information about other properties like the finding probability distribution of molecular orbital. The problem with the representation of multiple transparent isosurfaces [14] is that with the transparent body it is hard to perceive depth. A further disadvantage is that we cannot display another property in the same representation. Similarly as above the volume rendering technique also makes depth perception hard because of voxel transparency. The definition of depth perception is subjective, I used it in the context of comparing different types of representations. The point cloud representation with domain coloring is promising but until now it was not used in the field of molecular simulations.

## 2 Methods

Quantum mechanical models on their own are not suitable for describing the interaction of electromagnetic field and matter because of the exponential increase of dimension size. Classical models are usually unable to describe molecular phenomenon and in turn this can cause a marked discrepancy between measurement and simulation results. This is why I used a quantum mechanical model (Hartree-Fock or Density Functional Theory) for the description of the matter, the classical model for the electromagnetic field and semi-classical model for the interaction between them.

There is no such unified framework that would solve all these problems, so I relied on a combination of various programs. I used *ab initio* molecular modeling software such as GAMESS and NWChem for the simulation of molecular properties (electronic configuration, vibrational states, frequency-dependent polarizability) and the Finite Element Methods (FEM) module of CST Microwave Studio for the computation of classical electromagnetic field. Using the results of previous numerical calculations I implemented the semi-classical models in Matlab programming language. Paraview and VTK file formats were used for the stereoscopic visualization.

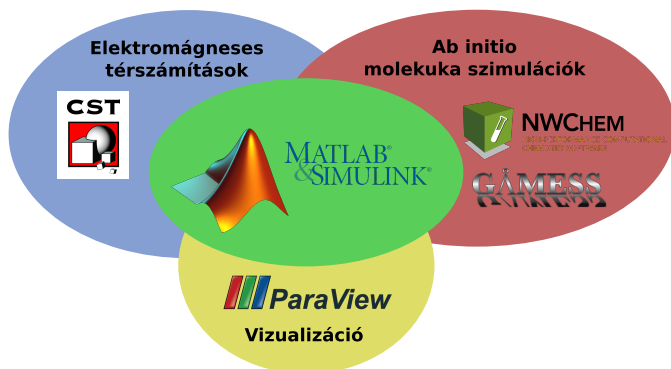


**Figure 2.1** – Different software was used for particular simulation tasks, and than Matlab framework was used to summarize the results.

## 3 New scientific results

### Thesis group I.

The Kretschmann type biosensor has three layers: optical, metal and molecular layer. For a specific arrangement we illuminate the metal surface through the optical layer with a laser beam in different incident angles and measure the reflection from the metal layer.

The plasmon resonance – which is an evanescent wave propagation of electrons in solids – evolves as a result of the proper wavelength, incident angle and p-polarization, and produces the reduction of reflection. The rate of plasmon resonance depends on the material of optics, the wavelength and incident angle of laser beam, the material and thickness of the metal layer and the time dependence of the molecular layer.

**1.1 I have given a numerical prediction to the specification of the Kretschmann type surface plasmon resonance biosensor for gases and dilute solvents using ab initio molecular simulation. The elaborated method makes it possible to design and optimize the parameters of the biosensor's excitation and the properties of the metal layer using classical electromagnetic field simulations. This method gives an opportunity to obtain better measurement results.**

*Related publications of the author: [1][3]*

I used *ab initio* molecular dynamics simulation to predict the frequency dependent complex dielectric function of the molecular layer. Using this method I determined the behavior of the sensor as a classical electromagnetic field. The frequency dependent dielectric function is determined by two main factors: the absorption capability of the molecules and the off-resonance polarizability of the electron configurations.

I have selected a frequency domain for the simulation of the absorption spectrum in which the probabilities of electronic transitions can be neglected, letting us to get a purely real dielectric constant [15, 16]. I used density functional theory for the calculation of frequency dependent polarizability.

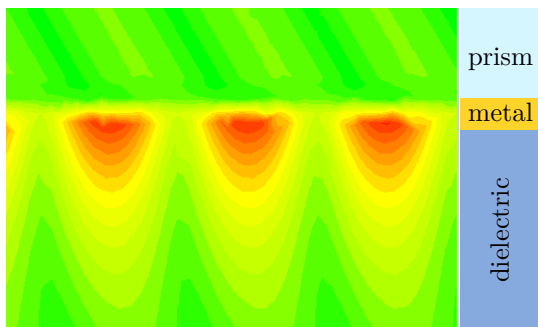


**Figure 3.1** – The absolute value of the electric field in the cross section of the biosensor.

I have modeled dilute solvents to avoid the interactions between molecules. For these solvents – as a first approximation – we can suppose that molecules equally fill the space, thus the value of polarizability is the average over different directions:  $\langle \alpha \rangle = 1/3(\alpha_{xx} + \alpha_{yy} + \alpha_{zz})$ . Although the susceptibility can be easily calculated with the formula  $\chi = N\alpha$ , I used the following model for liquids because of the amplification of dipole-dipole interactions:

$$\chi(\omega) = \frac{N\alpha(\omega)}{1 - (4\pi/3)N\alpha(\omega)}. \quad (3.1)$$

The linear dielectric function can be expressed as:

$$\varepsilon(\omega) = 1 + 4\pi\chi = \frac{1 + (8\pi/3)N\alpha(\omega)}{1 - (4\pi/3)N\alpha(\omega)}. \quad (3.2)$$

The dielectric function of water and ethanol that we can obtain by the above method at 632 [nm] is  $\varepsilon_{\text{water}} = 1.750$  and  $\varepsilon_{\text{ethanol}} = 1.841$ . For the description of gold metal layer I used Drude model ( $\varepsilon_{\infty} = 10$ ,  $\omega_p = 13.8 \cdot 10^{15}$  [Hz],  $\gamma = 1.075 \cdot 10^{14}$  [Hz]) which presents appropriate accuracy at optical wavelengths.

Using these dielectric constants I executed the finite element (“Frequency Domain Simulator”) simulation of classical electromagnetic field. There is no wave propagation in the perpendicular direction to the excitation and surface norm, thus I used the width of only one cell regarding to this direction, which

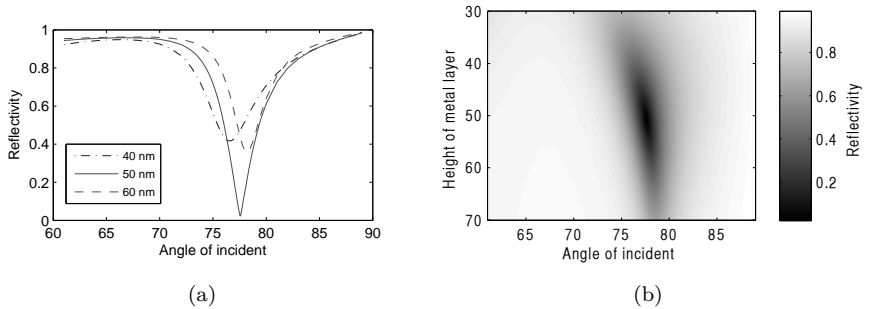


**Figure 3.2** – Plot (a) and contour plot (b) of sensor reflectivity in the function of incident angle and the thickness of the metal layer. The optimum is at about 50 nm thick metal layer.

can highly accelerate the simulation time. The configuration space in the other direction is approximately ten times as big as the current excitation wavelength.

I made optimization for the thickness of the metal layer at fixed excitation wavelength (632 [nm]) and fixed dielectric constant for the optical layer ( $\varepsilon_{prism} = 2.28$ ) with which we can get the ideal incident angle of the excitation. With this method I could model all aspects of the sensor’s behavior.

### 1.2 I have suggested a circuit model that enables a quick approximation for the design of the behavior of Kretschmann type biosensors.

Based on the analytical electromagnetic field solution of Kretschmann type biosensor, I created a transmission line model where the dielectric layers are related to the line segments [17]. For the specific layers the new, complex impedances are:

$$Z_0 = \frac{c}{\omega} \frac{\varepsilon_0}{\sqrt{\varepsilon_0 - k_0^2}}, \quad Z_1 = \frac{c}{\omega} \frac{\varepsilon_1}{\sqrt{\varepsilon_1 - k_0^2}}, \quad Z_2 = \frac{c}{\omega} \frac{\varepsilon_2}{\sqrt{\varepsilon_2 - k_0^2}}, \quad (3.3)$$

where  $k_0 = \sqrt{\varepsilon_0} \sin \theta$  and  $\theta$  is the angle of incidence.



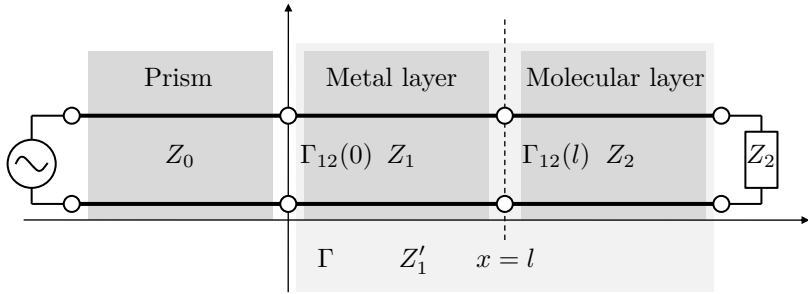


**Figure 3.3** – Equivalent transmission line model of Kretschmann type SPR biosensor.

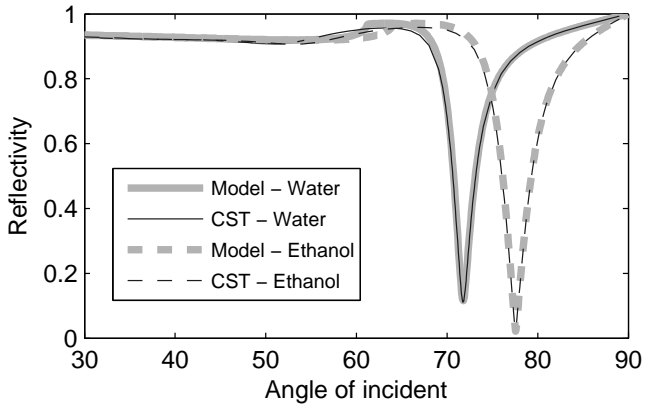


**Figure 3.4** – Comparison of transmission line model and CST numerical calculations. The reflectivity of exciting light is represented as a function of incident angle with different molecular layers (water, ethanol).

The calculation of the reflection – due to the monochromatic excitation – represents the behaviour of the biosensor:

$$\Gamma = \frac{\Gamma_{01} + \Gamma_{12}e^{-2j\beta l}}{1 + \Gamma_{01}\Gamma_{12}e^{-2j\beta l}}, \quad (3.4)$$

where  $\beta = -\frac{\omega}{c}\sqrt{\varepsilon_1 - \varepsilon_0 \sin^2 \theta}$  is the propagation constant,  $\Gamma_{01}$  and  $\Gamma_{12}$  are the reflection coefficients at the boundaries of different line segments.

Comparing the result of the equivalent circuit model and the numerical simulation we can conclude that the model describes correctly the different segments and gives an accurate prediction for the behavior of the biosensor. This new model is less general, thus significantly faster than the finite element method.

## Thesis Group II.

The main idea of the SEM is that the sample is excited with laser pulse and with a second laser pulse we force stimulated emission. The construction of the microscope can be seen in Fig. 3.5.

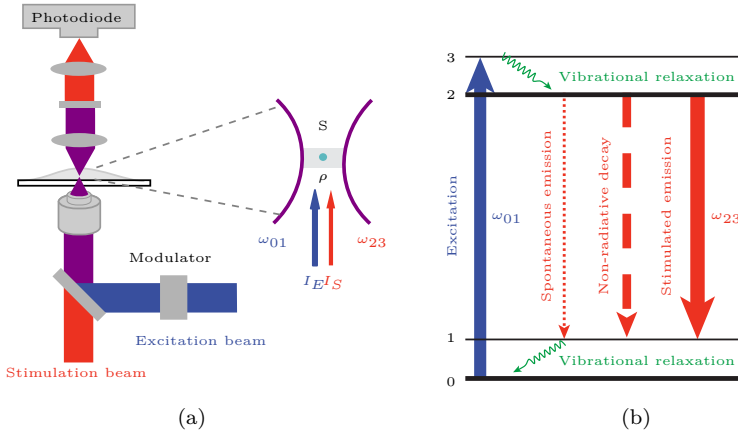


**Figure 3.5** – Schematic of the behaviour and experimental setup of stimulated emission microscope.

The behavior of the microscope can be discussed in two parts. As a result of the thermal bath – that is responsible for vibrational relaxation and spontaneous emissions – after the absorption of the molecules in the focus point the occupation probability of the excited states reduces and with the emission of photons jumps to lower energy states. We use light amplification instead of the fluorescence microscopy principles, namely we measure the intensity of the stimulated emission instead of the intensity of spontaneous emission caused by the excited molecules.

## **2.1 I have suggested a procedure for quantitative estimation of the behavior of the stimulated emission microscope using quantum-classical model and ab initio molecular dynamics simulations.**

*Related publications of the author: [2][4]*

I used semi-classical models for the simulation of the microscope’s behavior. The light was modeled as a classical electromagnetic field and the matter as a quantum mechanical system [18–23]. The effect of thermal bath (spontaneous emission, vibrational relaxations) and the time dependent dynamics of the occupation probability of the states were defined by Liouville-von Neumann equations. Although only a few molecules can be found in the volume of excitation, we can not suppose statistical ensemble, but because we prepare the measurements multiple times we can use density matrix formalism as a prediction of time average.

I used the Born-Oppenheimer approximation in the quantum mechanical model to separate the electron and nuclear components. For the electronic configuration I took into account the ground and the first excited state, however for the vibrational state I used the quantum harmonic oscillator model which is a good first order approximation. We can neglect the interaction between the vibrational states.

Due to the large number of photons we can use classical electromagnetic model for the description of excitation beam and because the wavelength of the excitation is much larger than the size of the molecule we can use electric dipole approximation ( $H_{int} = -\mathbf{d} \cdot \mathbf{E}$ ) for the interaction of the field

and matter. All of the interactions are weak, thus they do not change the eigenstates of the closed system.

A master equation that describes an arbitrary molecule is not necessarily solvable because of the large number of modes and their states; however we can calculate that the pulses used for excitation are large enough (more than 100 fs) and that vibrational modes are independent. This way we can reduce the simulation space to the state transitions that are the most dominant describing the process. I used an idealised model to determine the possible state transitions. Although the model used is quite simple it includes the description of excitation and emission processes, and gives us a first order approximation for the absorption and emission spectrum.

If the interaction of the pulses happens between different modes the spontaneous emission will have the most significant role. The most important case from all possible state transitions is when the two excitations interact with state transitions belonging to the same vibrational modes:

$$\omega_e = \omega_a + \omega_v, \quad \omega_s = \omega_a - \omega_v. \quad (3.5)$$

According to the above principles the Hamiltonian that describes the full system:

$$\mathbf{H}(t) = \mathbf{H}_{sys} + \mathbf{H}_{env} + \mathbf{H}_{sys-env} + \mathbf{H}_e(t) + \mathbf{H}_s(t), \quad (3.6)$$

consists of the closed system's Hamiltonian ( $\mathbf{H}_{sys}$ ), environment's Hamiltonian ( $\mathbf{H}_{env}$ ), the system-bath interaction's Hamiltonian ( $\mathbf{H}_{sys-env}$ ) and the Hamiltonian related to the excitation ( $\mathbf{H}_e(t)$ ) and the stimulated emission ( $\mathbf{H}_s(t)$ ). The above operators can be expressed as follows:

$$\mathbf{H}_{sys} = \frac{1}{2} \hbar \omega_a \sigma_z + \hbar \omega_v a_v^\dagger a_{v_j}, \quad (3.7)$$

where  $\omega_a = (E_e - E_g)/\hbar$  is the frequency of electronic transition,  $\sigma_z$  is the Pauli operator,  $\omega_{v_j}$  is the frequency of vibrational state and finally  $a_{v_j}^\dagger$  and  $a_{v_j}$  are the creation and annihilation operators. Assuming single photon excitation the state transitions for the electronic and vibrational states are the following:

$$\mathbf{H}_e(t) = -\mathbf{d} \cdot \tilde{\mathbf{E}}_e(t) = -d_{ij} S \tilde{\mathbf{E}}_e(t), \quad (3.8)$$

$$\mathbf{H}_s(t) = -\mathbf{d} \cdot \tilde{\mathbf{E}}_s(t) = -d_{ij} S \tilde{\mathbf{E}}_e(t), \quad (3.9)$$

$$S = (\sigma_+ + \sigma_-) \cdot (a_v^\dagger + a_v), \quad (3.10)$$

where  $\sigma_+$  and  $\sigma_-$  are the Pauli operators for the electric transition,  $d_{ij}$  is the transition dipole moment for states  $i$  and  $j$ .

The classical electromagnetic fields ( $\tilde{E}_s$ ,  $\tilde{E}_e$ ) of the excitations can be determined as follows:

$$\tilde{E}_s(t) = \text{Re}[A_s(t)E_{0,s}e^{-j\omega_s t}] = A_s(t)\frac{1}{2}E_{0,s}(e^{-j\omega_s t} + e^{j\omega_s t}), \quad (3.11)$$

$$\tilde{E}_e(t) = \text{Re}[A_e(t)E_{0,e}e^{-j\omega_e t}] = A_e(t)\frac{1}{2}E_{0,e}(e^{-j\omega_e t} + e^{j\omega_e t}), \quad (3.12)$$

where  $E_{0,s}$  and  $E_{0,e}$  are the peak intensities of the electric fields,  $A_s$  and  $A_e$  are the envelope of laser pulses, that can be expressed as follows accordingly:

$$A_s(t) = e^{-4 \ln 2 \frac{(t-t_{0,s})^2}{2\tau_s^2}}, \quad A_e(t) = e^{-4 \ln 2 \frac{(t-t_{0,e})^2}{2\tau_e^2}}, \quad (3.13)$$

where  $t_{0,s}$  and  $t_{0,e}$  are the time delays and finally  $\tau_s$  and  $\tau_e$  are the full width at half maximum of the pulses.

Introducing the Rabi frequencies:

$$\Omega_{ij,e} = \frac{d_{ij}E_{0,s}}{\hbar}, \quad \Omega_{ij,s} = \frac{d_{ij}E_{0,e}}{\hbar}, \quad (3.14)$$

we can determine the operator of interaction in the following form:

$$H_e(t) = -\hbar\Omega_{ij,e} S A_e(t)\frac{1}{2}(e^{-j\omega_e t} + e^{j\omega_e t}). \quad (3.15)$$

$$H_s(t) = -\hbar\Omega_{ij,s} S A_s(t)\frac{1}{2}(e^{-j\omega_s t} + e^{j\omega_s t}). \quad (3.16)$$

Taking into account the effect of the environment and supposing a single vibrational state the master equation of the system is the following:

$$\begin{aligned} \frac{d}{dt}\rho = & -\frac{i}{\hbar} [H_{sys} + H_e(t) + H_s(t), \rho] \\ & + \gamma \left( \sigma_+ \rho \sigma_- - \frac{1}{2} \sigma_- \sigma_+ \rho - \frac{1}{2} \rho \sigma_- \sigma_+ \right) \\ & + \kappa_v (1 + n_v^{(th)}) \left( a_v \rho a_v^\dagger - \frac{1}{2} a_v^\dagger a_v \rho - \frac{1}{2} \rho a_v^\dagger a_v \right) \\ & + \kappa_v n_v^{(th)} \left( a_v^\dagger \rho a_v - \frac{1}{2} a_v a_v^\dagger \rho - \frac{1}{2} \rho a_v a_v^\dagger \right), \end{aligned} \quad (3.17)$$

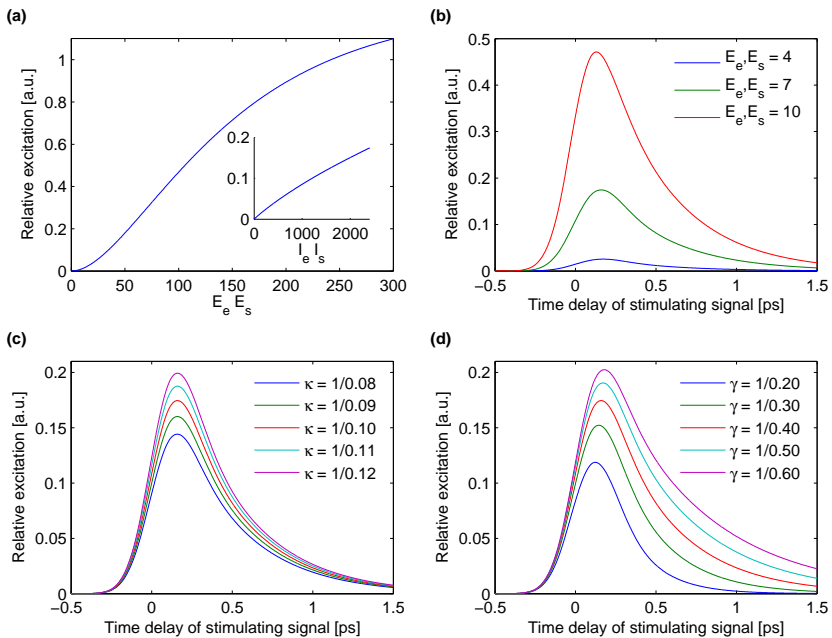


**Figure 3.6** – Numerical results of the model: (a) shows the relative excitation as a function of the two excitation signal amplitude’s product using a fixed ( $t_{0,s} = 0.15$  [ps]) delay. The effect of the two excitation signal’s amplitude (b), the rate of the vibrational relaxation (c) and the rate of excited state relaxation (d) are shown as a function of time delay. ( $\lambda_a = 618.5$  [nm],  $\lambda_v = 782$  [cm $^{-1}$ ],  $\gamma = 1/0.4$ ,  $\kappa_v = 1/0.1$ ,  $\lambda_e = 590$  [nm],  $\lambda_s = 650$  [nm],  $\Omega_e, \Omega_s = 7$ ,  $\tau_e, \tau_s = 0.2$  [ps])

that consists of the effect of spontaneous emission and the excitations and emissions – that determine the vibrational relaxations – of the vibrational states.

The time evolution of the model shows that the molecules come to excited state as a result of the laser pulse. As a consequence of the second laser pulse – besides the continuous vibrational relaxation and spontaneous emission – the excited molecules get back to ground state producing additional photons by stimulated emission.

Fig. 3.6 shows the evaluation of stimulated emission as a function of the product of the intensity of the two pulses. We can obtain that initially the rate of stimulated emission grows linearly. The dynamics of time evolution depends mostly on the relaxation ( $\kappa$ ,  $\gamma$ ) and excitation parameters. Increasing the vibrational relaxation ( $\kappa$ ), the relaxation happens very fast and thus at the evolution of stimulated emission spontaneous emission is the most dominant phenomenon that happens much slower. The increase of the spontaneous emission factor ( $\gamma$ ) results in the decrease of stimulated emission intensity.

The constructed model determines the behavior of the microscope as published; however to precisely determine the parameters we need further measurements. As a function of the delay between excitations the rate of stimulated emission can be determined in a molecule specific manner – based on the vibrational and spontaneous emission’s coefficients in the excited state. This gives us the opportunity to use the principles of stimulated emission microscopy for molecule detection.

## Thesis Group III.

The existing methods for three dimensional visualization are capable of amazing representation, however using stereoscopic display system the perception of depth does not evolve because of the applied transparency.

**3.1 Combining existing techniques like point cloud and domain coloring I have developed a new visualization method of complex wave functions that can be used efficiently for stereoscopic display systems.**

*Related publications of the author: [5]*

Given a complex wave function that describes the behavior of the system (a photon, electron or molecule), the selected part of the whole system (like an electron configuration in the case of a molecule) is calculated on a uniformly spaced grid structure.

The points represented were generated according to their finding probabilities. I have developed a points generation algorithm based on locally overlap-

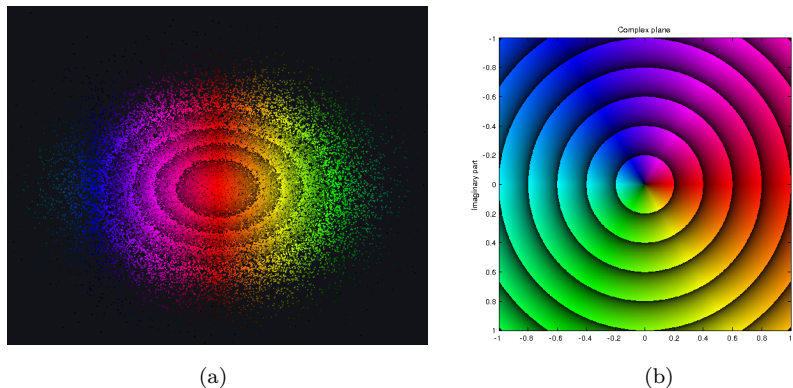


**Figure 3.7** – Cross section of the wave packet (a) and its colormap (b).

ping triangular distribution. Function values are determined by interpolation and represented by colors based on a selected domain coloring technique. The density of the points is proportional to the finding probability so we can represent other properties (i.e. phase information) by the coloring technique. We have the opportunity to filter and cut off the area of interest in real time due to the new generation of video cards. Additionally the new method uses the advantages of stereoscopic display systems.



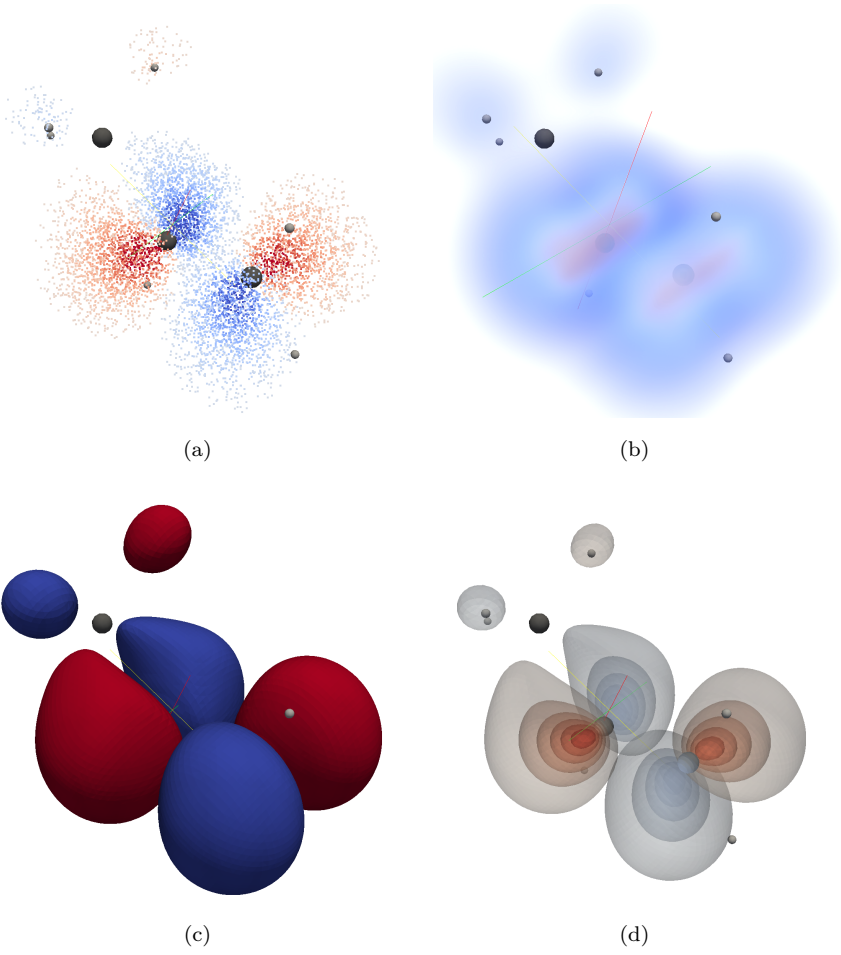


**Figure 3.8** – Comparison of three dimensional visualizations: (a) point cloud, (b) volume rendering, (c) isosurface and (d) multiple transparent isosurfaces.

## 4 Application of the results

The use of SPR based biosensors made it possible to perform fast and accurate medical diagnostic examinations. These biosensors became more accurate by computer-aided design. This lets us use more and more molecule-specific sensors and helps to further increase the usage of SPR biosensors in medical diagnostics.

I have shown that the behaviour of surface plasmon resonance biosensors can be explained using the combination of classical electromagnetic field theory and modern numerical simulations, and that these techniques can be used for parameter optimization. By refining the model we have the opportunity of designing computer-aided sensors that can make it easier to carry out experiments quickly and accurately.

We have the possibility to examine biologically relevant processes that we were unable to characterize using previous techniques with the understanding of the basic phenomenon of stimulated emission microscopy. We can carry out “in vivo” measurements without fluorescence labeling – for example by endoscopy –, we can examine the rate or the time dependence of molecules of our interest [11] and furthermore we can get closer to the direct monitoring of biological processes. These are the main reasons why we have to understand the boundaries, opportunities and the quantitative behaviour of stimulated emission microscopes.

Data representation in three dimensional space has a significant practical advantage. Nowadays we have the opportunity to process large amount of data, thus it became important to have a tool in our hand that helps us represent the information accurately.

## 5 Acknowledgments

First of all I would like to say thank to my supervisor, *Prof. Árpád Csurgay* for his guidance and for our unforgettable discussions that helped me a lot and gave me a lot strength during my work.

I thank to *Prof. Tamás Roska* and *Prof. Péter Szolgay* former and current Head of the Doctoral School for their advice, encouragement and the inspiration for the multidisciplinary approach. Furthermore, I am thankful for the work of the administrative and financial staff of the Faculty that ensured the conditions during my whole work.

Special thanks goes to my colleagues at the Doctoral School – Imre Juhász, Gergely Treplán, Ádám Rák, Andrea Kovács, Dávid Tisza, Péter Vizi, Zoltán Kárász, László Füredi and Tamás Pilissy – for the professional discussions and for their friendship.

And finally I would like to thank the support of my family and special thanks goes to Dóra Bihary for her encouragement.

# List of Publications

## Journal publication of the author

- [1] A. Fekete, “Simulation of absorption-based surface plasmon resonance sensor in the Kretschmann configuration”, *International Journal of Circuit Theory and Applications*, vol. 41, no. 6, pp. 646–652, 2013.
- [2] A. Fekete and A. I. Csurgay, “A computational model for label-free detection of non-fluorescent biochromophores by stimulated emission”, *Biomedical Optics Express*, vol. 6, no. 3, pp. 1021–1029, 2015.

## Conference and laboratory publications

- [3] A. Fekete, “Simulation of Absorption Based Surface Plasmon Resonance Sensor in the Kretschmann Configuration”, *Proceedings of the Multidisciplinary Doctoral School*, pp. 117–120, 2011.
- [4] I. Juhász, A. Fekete, and A. I. Csurgay, “Two-photon and Stimulated Emission Microscopy - Quantum Electrodynamics in Simulations”, in *Bionics: At the crossroads of Biotechnology and Information Technologies*, 2013.
- [5] A. Fekete, “A First-Principle Computational Model for Electronic Structure of Molecular or Atomic Media”, *Proceedings of the Multidisciplinary Doctoral School*, pp. 21–24, 2009.

## References

- [6] A. I. Csurgay and W. Porod, “Surface plasmon waves in nanoelectronic circuits”, *International Journal of Circuit Theory and Applications*, vol. 32, no. 5, pp. 339–361, 2004.
- [7] J. Homola, “Surface plasmon resonance sensors for detection of chemical and biological species.”, *Chemical reviews*, vol. 108, no. 2, pp. 462–93, 2008.
- [8] S. A. Maier, *Plasmonics: Fundamentals and Applications*. Springer, 2007.
- [9] L. Novotny and B. Hecht, *Principles of Nano-Optics*. Cambridge University Press, 2006.
- [10] W. Min, S. Lu, S. Chong, R. Roy, G. R. Holtom, and X. S. Xie, “Imaging chromophores with undetectable fluorescence by stimulated emission microscopy.”, *Nature*, vol. 461, no. 7267, pp. 1105–9, 2009.
- [11] S. W. Hell and E. Rittweger, “Microscopy: Light from the dark.”, *Nature*, vol. 461, no. 7267, pp. 1069–70, 2009.
- [12] D. R. Lipşa, R. S. Laramée, S. J. Cox, J. C. Roberts, R. Walker, M. a. Borkin, and H. Pfister, “Visualization for the Physical Sciences”, *Computer Graphics Forum*, vol. 31, no. 8, pp. 2317–2347, 2012.
- [13] B. Thaller, *Advanced Visual Quantum Mechanics*. Springer, 2004.
- [14] Y. Jang and U. Varetto, “Interactive volume rendering of functional representations in quantum chemistry.”, *IEEE transactions on visualization and computer graphics*, vol. 15, no. 6, pp. 1579–1586, 2009.
- [15] A. Szabó and N. S. Ostlund, *Modern Quantum Chemistry: Introduction to Advanced Electronic Structure Theory*. Dover Publications, 1989.
- [16] D. Marx and J. Hutter, *Ab Initio Molecular Dynamics: Basic Theory and Advanced Methods*. Cambridge University Press, 2009.
- [17] K. Simonyi and L. Zombory, *Elméleti villamosságatan*. Műszaki Könyvkiadó, 2000, p. 834.

- [18] A. Csurgay, K. Simonyi, and I. Dr. Lovas, *Az információtechnika fizikai alapjai*. BME Mérnöktoábbképző Intézet, 1997, p. 636.
- [19] D. P. Craig and T. Thirunamachandran, *Molecular Quantum Electrodynamics*. Dover Publications, 1984.
- [20] H.-P. Breuer and F. Petruccione, *The Theory of Open Quantum Systems*. Oxford University Press, 2002.
- [21] M. O. Scully and M. S. Zubairy, *Quantum Optics*. Cambridge University Press, 1997.
- [22] G. Grynberg, A. Aspect, C. Fabre, and C. C. Tannoudji, *Introduction to Quantum Optics: From the Semi-Classical Approach to Quantized Light*. Cambridge University Press, 2010.
- [23] H. Carmichael, *An Open Systems Approach to Quantum Optics: Lectures Presented at the Université Libre De Bruxelles, October 28 to November 4, 1991*. Springer, 1993.